AIAA 81-4259

Boundary-Layer Flow at an Air-Water Interface with Spray Entrainment

J. Michael Macha* and David J. Norton†
Texas A&M University, College Station, Texas

The effect of spray entrainment on the mean wind profile above a wavy water surface has been treated by including an additional spray stress term in the log law for turbulent boundary-layer flow. The results of measurements in a high-speed wind/wave channel support the modified log law and the partitioning of the vertical momentum flux between separation drag on the wave shape and acceleration of entrained water drops. An existing correlation for the log law roughness parameter for solid boundaries is shown to apply to the wavy water surface. At the maximum channel wind speed of 25 m/s, the drag force on the spray accounted for 30-35% of the momentum flux into the shear layer.

Introduction

WIND loads are an important consideration in the design of marine structures. For designs with large plan areas exposed to the wind or with superstructures which rise to several hundred feet above the water surface, the wind load may account for a significant part of the total overturning moment.[1] Since this force is proportional to the square of the wind speed and since the wind speed varies with altitude, the design engineer must select a suitable model for the wind field. Of primary interest is the extreme condition of hurricane force winds (>34 m/s) with wave heights of the order of the structure's clearance above the mean water level. In this situation the interactions at the air-water boundary cannot be ignored, and a relatively unstudied phenomenon becomes important: the entrainment of large amounts of sea spray and the attendant transfer of momentum to the accelerating water drops results in a modification to the wind field. This paper is concerned with the effect of entrained spray on the mean wind profile, which is the usual design velocity for wind load calculations.

Current industry practice[2] is to use the power law model $\langle u\rangle \sim z^n$, where $\langle u\rangle$ is the mean wind velocity and z the vertical coordinate originating at the mean water level. This model is well established for the atmospheric boundary layer (ABL) over land, where the exponent n has been correlated with terrain (wheat field, forest, urban area, etc.).[3] However, the problem with applying the power law profile to the marine ABL is that the single parameter n cannot adequately describe the complex, interacting geometry of the sea surface or the spray content of the air.

An alternative to the power law is suggested by the observation[4] that in the lowest 10% of the marine ABL, the mean wind obeys the "log law" formulation which has been developed for aero- and hydrodynamic flows over solid rough surfaces.

The purpose of this paper is to present a modified log law formulation for the mean wind over a wavy water surface, including the effect of spray entrainment on the momentum balance within the shear layer. The model is compared to data taken in a high-speed wind/wave channel. The ultimate goal of this line of research is an engineering model for the wind field adjacent to the sea surface during extreme wind conditions.

Received March 17, 1980; revision received Dec. 8, 1980.

*Currently Assistant Professor, Aerospace Engineering and Engineering Mechanics Department, The University of Texas, Austin. Member AIAA.

†Associate Professor, Aerospace Engineering Department. Associate Fellow AIAA.

Formulation of the Modified Log Law

The Logarithmic Layer

The log law for turbulent flow past a solid boundary composed of two-dimensional roughness elements oriented normal to the wind can be expressed as[5]

$$\frac{\langle u\rangle}{u_*} = \frac{1}{\kappa}\ln\frac{z}{h} + A(\lambda, R_r) \tag{1}$$

Here $u_* = \sqrt{\tau_w/\rho}$ is the friction velocity, h the vertical dimension of the roughness elements, and κ von Kármán's proportionality factor between the turbulent mixing length and distance from the boundary. The wall shear stress τ_w is the drag per unit area at the boundary and is due primarily to local flow separation from individual roughness elements, with a minor contribution from surface friction in the attached-flow regions. The roughness parameter $A(\lambda, R_r)$ characterizes the type of roughness and the state of development of the flow. It is a function of the roughness density $\lambda = p/h$ where p is the streamwise spacing of roughness elements and the roughness Reynolds number $R_r = u_* h/\nu$. For R_r greater than some critical value, the dependence on R_r vanishes and the flow is referred to as fully rough. However, the dependence on λ remains and has been the subject of numerous experimental investigations.[6-9] The recent study by Han et al.[9] found the correlation

$$A(\lambda,\phi) = 3.30 - \frac{(\lambda/10)^n}{(\phi/90\ \text{deg})^{0.35}} \qquad n = \begin{cases} -0.13, & \lambda < 10 \\ +0.53, & \lambda \geq 10 \end{cases} \tag{2}$$

to be valid for a roughness geometry described by λ and the angle ϕ defined in Fig. 1. For a particular value of the angle ϕ, the roughness function is minimum for $\lambda = 10$. Referring to Eq. (1), this roughness density corresponds to the condition of maximum surface drag.

The possibility that Eq. (2) can be applied to a wavy water surface is suggested by the data of Beebe and Cermak[10] for solid, sinusoidal waves. Those data are well fit by Eq. (2) if $\phi = \arctan(2H/L)$, where H and L are the wave height and wavelength, respectively. This result is compatible with the contention that surface drag is dominated by flow separation from the crests of the roughness elements.

Spray Entrainment

Sea spray is observed to appear at a threshold wind velocity of 10–15 m/s, and the amount of entrained water increases much faster than linearly with velocity.[11,12] However, there are no quantitative sea spray concentration data available for wind speeds greater than about 20 m/s. Qualitatively, the air

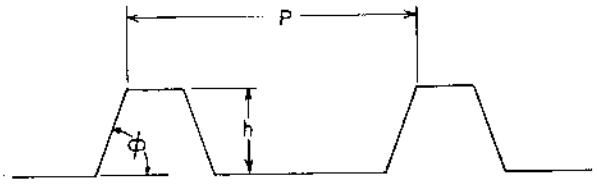

Fig. 1 Roughness geometry of Han et al.[9]

above the sea surface during hurricane winds has been described by Kraus[11] as "too thin to swim in but too thick to breathe."

Considering that a spray drop is ejected into the wind vertically and then accelerated horizontally, it becomes a sink for the wind's streamwise momentum. The rate at which momentum is transferred to the drop represents a drag force, which appears in the time-averaged boundary-layer equation

$$u\frac{\partial u}{\partial x}+w\frac{\partial u}{\partial z}=-\frac{1}{\rho}\frac{\mathrm{d}P}{\mathrm{d}x}+\frac{1}{\rho}\frac{\partial}{\partial z}(\tau_{xz})-\frac{1}{\rho}X_s \qquad (3)$$

as the term X_s. This spray drag per unit volume can be expressed as

$$X_s=\sum_i\sum_j N_{ij}(1/2\rho A p_i)C_{D_{ij}}(u-u_{p_j})^2 \qquad (4)$$

where the overbar indicates a time average, u_p is the horizontal drop velocity, C_D the aerodynamic drag coefficient of the drop, and $A_p=\pi d^2/4$ where d is the diameter of a spherical drop. N_{ij} is the number concentration of drops of size i and speed j, and the summations are over all sizes and speeds.

If Eq. (3) is integrated from the surface to some altitude δ which is outside both the wind shear and spray layers, then the last two terms on the right side of the equation become

$$\frac{1}{\rho}\int_0^\delta\left(\frac{\mathrm{d}\tau_{xz}}{\mathrm{d}z}-X_s\right)\mathrm{d}x=-\frac{1}{\rho}(\tau_0+\tau_s) \qquad (5)$$

The term τ_0 is the familiar term of the integral form of the boundary-layer equation and represents the surface stress due primarily to local separation from the wave crests. The term τ_s is introduced and defined as the integral of the spray drag force X_s. It represents the additional drag due to spray in a unit vertical column extending upward from the surface. It can be argued that most of the contribution to the integral occurs near the surface where both drop concentration N and relative velocity $(u-u_p)$ are large. Thus, to an approximation, τ_s can be treated as an additional surface stress term.

In the logarithmic portion of the boundary layer, the friction velocity represents the total momentum flux to the surface. Thus, a log law for the mean wind velocity relative to the moving waves, including the effect of spray entrainment, can be written as

$$\frac{\langle u-c\rangle}{u_*}=\frac{1}{\kappa}\ln\frac{z}{H}+A(\lambda)+B_s \qquad (6)$$

where c is the wave speed and the roughness parameter $A(\lambda)$ is given by Eq. (2) with $\lambda=L/H$ and $\phi=\arctan(2/\lambda)$. Considering the previous arguments concerning τ_0 and τ_s, the friction velocity becomes

$$u_*=\left[\frac{\tau_0+\tau_s}{\rho}\right]^{1/2} \qquad (7)$$

The additive term B_s represents an increase in the "aerodynamic roughness" of the water surface due to the production of spray drops. This effect is illustrated qualitatively in Fig. 2, where both the slope and the z_0 intercept of the curve are modified by entrainment. A functional form for B_s is suggested by experimental results to be discussed subsequently.

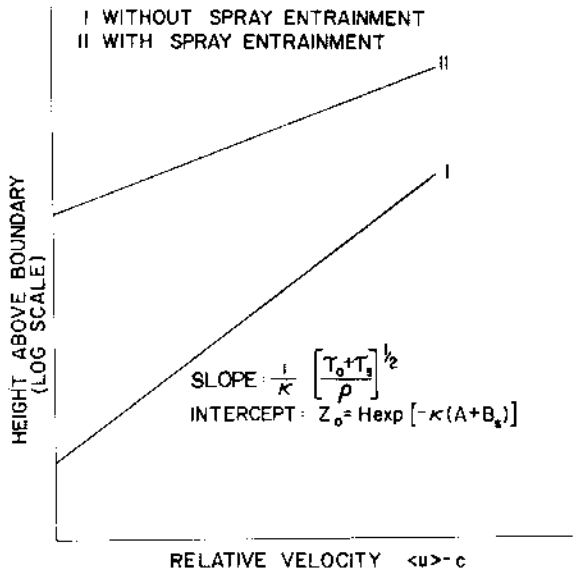

Fig. 2 Effect of spray entrainment on the log law.

von Kármán's κ

The results of several experimental investigations involving two-phase flows suggest that the value of κ for flow above a water surface with appreciable spray entrainment may be less than the pure fluid value of about 0.4. Perskin and Wallace (see Ref. 13, p. 86) investigated the turbulence structure of airflow in a pipe, with and without the injection of 0.1 mm diam glass beads. The results indicate a 22% decrease in the average intensity of turbulent velocity fluctuations for a mass loading of approximately 1×10^{-3} g/cm^3. The fluctuations are directly related to the turbulent mixing length ℓ so that a reduction in intensity is accompanied by a reduction in ℓ. Since $\ell=\kappa z$, it is expected that at a fixed distance from the boundary the value of κ is also reduced.

Most of the data on this topic are from studies in the field of sediment transport. Numerous investigators have measured suspended sediment concentrations, mean velocity profiles, and head loss in both laboratory channels and actual waterways. Several data sets were compiled by Einstein and Chien.[14] The factor κ was correlated with a ratio of powers, P_s/P_τ. In the present notation,

$$P_s=\frac{\rho_w-\rho}{\rho_w}gw_s\int_0^\delta\rho_s\,\mathrm{d}z \qquad (8)$$

is the power required to maintain the mass concentration of spray particles ρ_s in suspension. The settling velocity of the spray is w_s and g is gravitational acceleration. Again, δ is some height above the spray layer, ρ the air density, and ρ_w the density of water. This power is provided by the turbulent mechanical energy associated with the wind shear and the total available power can be expressed as

$$P_\tau=\int_0^\delta(\tau_0+\tau_s)\frac{\partial u}{\partial z}\,\mathrm{d}z=\tau_w u_\delta \qquad (9)$$

where $\tau_w=\tau_0+\tau_s$. According to the correlation of Ref. 14 which is shown here as Fig. 3, a suspended load of droplets equivalent to about 2% of the available turbulent energy would reduce the value of κ by 25%, to $\kappa=0.3$. A spray load equivalent to 10% would reduce κ to a value of 0.2.

The Effective Wave Height

Equation (6) was developed for a water surface made up of a single-component wave shape of height H and phase speed c. More realistically, a wavy water surface contains a range of wave shapes and is best described by the frequency spectrum

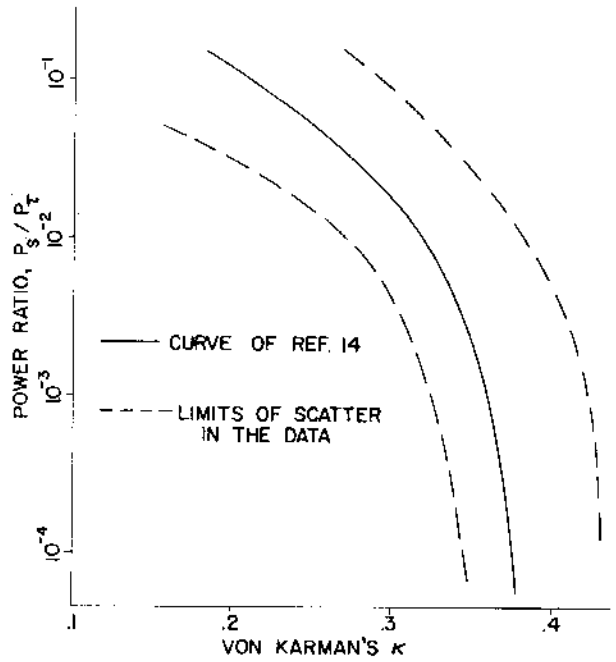

Fig. 3 Variation of von Kármán's κ with suspended particle concentration.

of the water level displacements $S(f)$, where

$$\sigma^2 = \int_0^\infty S(f)\,df \tag{10}$$

and σ^2 is the variance of the displacements. The exact shape of $S(f)$ is a complex function of wind speed, water depth, fetch, and wind duration. Furthermore, each component of the wave spectrum propagates at its own phase speed, making the selection of H and c ambiguous.

Wave speed may be taken inside the argument of the logarithm in Eq. (6), with the result that H is replaced by an effective height

$$H_c = H\exp(-\kappa c/u_*) \tag{11}$$

Kitaigorodskii[15] has suggested the following expression for H_c for the sea surface:

$$H_c = 2\sqrt{2}\left[\int_0^\infty S(f)\exp(-2\kappa c/u_*)df\right]^{1/2} \tag{12}$$

Here, the wave speed is a function of wave frequency f, and is given by the deep water relationship $c = g/2\pi f$ for components with wavelengths less than about one-half of the mean water depth. For a single component spectrum, Eq. (12) reduces to Eq. (11), with

$$H = \overline{H} = 2\sqrt{2}\sigma \tag{13}$$

$\overline{H}$ is known as the significant wave height and, for a pure sinusoidal surface, it is equal to twice the amplitude of the sinusoid.

The integral in Eq. (12) could be evaluated numerically for a specified design wave spectrum. However, since the exponential contains the unknown friction velocity, an iterative procedure with the log law would be required. For an actively developing sea, with high-wind speed and large surface stress, Kitaigorodskii[15] suggests using

$$H_c = \overline{H}\exp(-\kappa c_0/u_*) \tag{14}$$

where c_0 is the phase speed of the component with the peak spectral energy density. This expression closely approximates Eq. (12) if $S(f)$ contains a strongly-dominant spectral component.

Measurements in a Wind/Wave Channel

Description of the Wind/Wave Channel

Measurements of the wind velocity, spray content of the wind, and instantaneous water surface displacements were conducted in a wind/wave facility designed specifically for this investigation and located in the Texas A&M University Hydromechanics Laboratory. Air is drawn through the 20 cm wide by 44 cm deep by 11 m long channel by a centrifugal-type air mover driven at constant rpm by an electric motor. Air velocity is controlled by an adjustable vent at the entrance to the compressor and by a variable-area exhaust section. An adjustable plate provides a smooth transition between the air inlet and the water surface. The downwind end of the channel has a sloping beach of fibrous material which effectively absorbs the wind-generated waves. The channel has an adjustable tilt of up to 0.014/1 from the horizontal which was used to counter the water surface setup and reduce the pressure gradient in the direction of airflow. The primary test section was located at a fetch of 6.0 m downstream from the transition plate. For a nominal water depth of 15 cm, the maximum wind speed was about 25 m/s with wave heights of 6 cm. Details of the experimental facility and procedure may be found in Ref. 16.

Wave Measurements

The basic instrument used for water level measurements was a capacitance-type wave gage and amplifier/recorder system. For each wind condition, the root mean square (rms) of the output signal was measured on line with a true rms voltmeter. The mean level of the water surface was found within ± 1.0 mm by low pass filtering the signal with a cutoff frequency below that of the dominant wave. In addition, the unfiltered signal was recorded on FM magnetic tape for subsequent spectral analysis. Estimates of the frequency spectral energy density of the surface displacement were computed from digitized samples of the recorded signal using the FFT procedure described by Welch.[17] A dominant wave frequency for each wind condition was determined from the spectra.

Wind-driven waves propagate at a speed that is the sum of the wave celerity and a surface drift velocity due to the shearing stress at the air-water interface. In the present study, the following procedure was used to determine this resultant wave speed. A time-lag cross correlation was performed on the output of two wave gages positioned a short distance (11.50 cm) apart. The gage separation distance divided by the time-lag for maximum correlation defined a statistically averaged speed for the dominant wave. Then, the wave length was established by dividing the wave speed by the wave frequency.

The last three columns of Table 1 summarize the wave measurements for the range of wind speeds included in the experiment. The mean wind speed $\overline{u}$ represents a spatial average of $\langle u(z)\rangle$ over the height of the channel and the significant wave height $\overline{H}$ is defined as the rms of the surface displacements multiplied by the factor $2\sqrt{2}$. In addition to the quantitative measurements, still photography and high-speed movies were used to document the development of wave shapes and the generation and transport of spray. The photographic data are presented in Ref. 16.

Wind Velocity Measurements

The mean wind velocity in the channel was measured with a total-static pressure probe. Due to the amount of spray produced at the higher wind speeds, ordinary small-orifice probes were frequently fouled by water ingestion and gave erroneous results. This problem was overcome by designing oversized (0.95 cm diam) total and static probes which were self-clearing. Water captured by the total probe was scavenged through a small orifice at the rear, with an error in stagnation pressure as a result of flow through the probe of less than 0.5% of the freestream dynamic pressure. Self-clearing of the static probe was insured by making the orifices sufficiently large (0.476 cm diam).

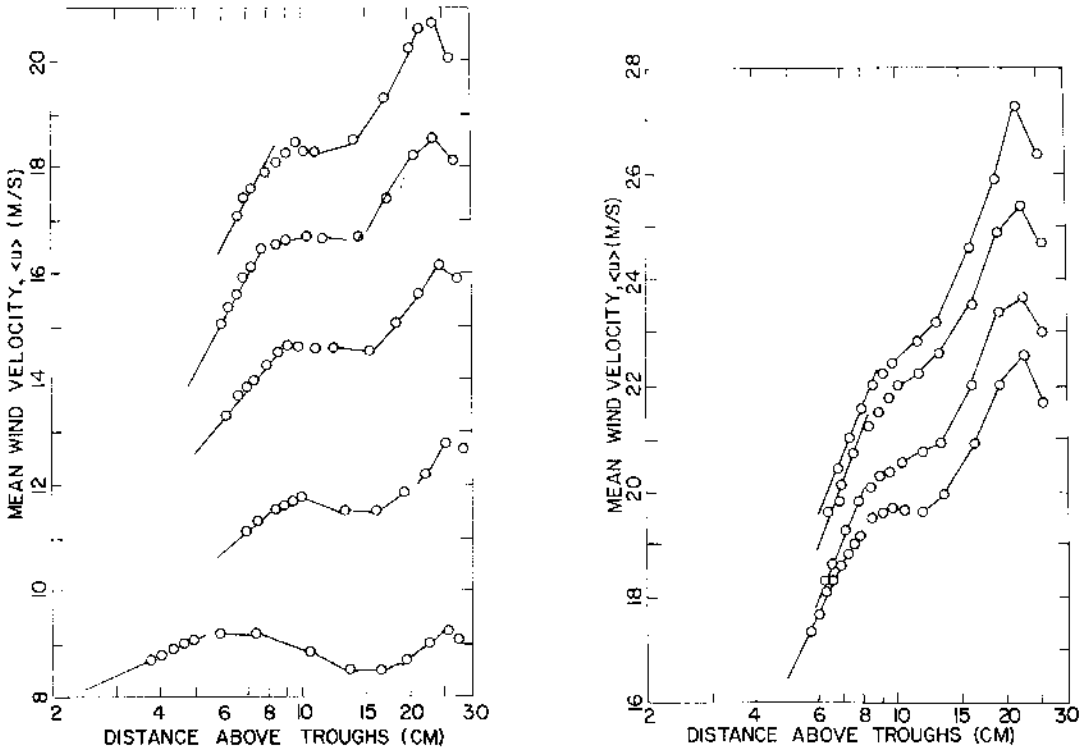

Fig. 4 Mean velocity profiles above air-water interface.

Table 1 Summary of wind/wave data

$\bar{u}$, m/s	u_{10}, m/s	(u_*/κ) m/s	z_0, cm	$(u_*/u_{10})^2$ $(\times 10^3)$	c_0, m/s	$\bar{H}$, cm	L, cm
7.7	16.5	1.39	7.2×10^{-3}	1.14	0.87	3.02	37.5
10.6	23.8	2.54	8.7×10^{-2}	1.83	1.00	4.58	54.0
13.3	31.5	3.56	0.15	2.05	1.08	4.92	59.5
15.5	42.0	5.25	0.34	2.50	1.09	5.18	60.5
17.1	47.0	5.96	0.38	2.58	1.10	5.35	63.5
18.2	50.1	6.34	0.37	2.57	1.13	5.52	75.2
18.9	53.8	7.00	0.46	2.71	1.16	5.66	77.5
19.8	57.3	7.49	0.48	2.74	1.21	5.66	88.0
20.2	56.7	7.28	0.41	2.63	1.23	5.77	90.3

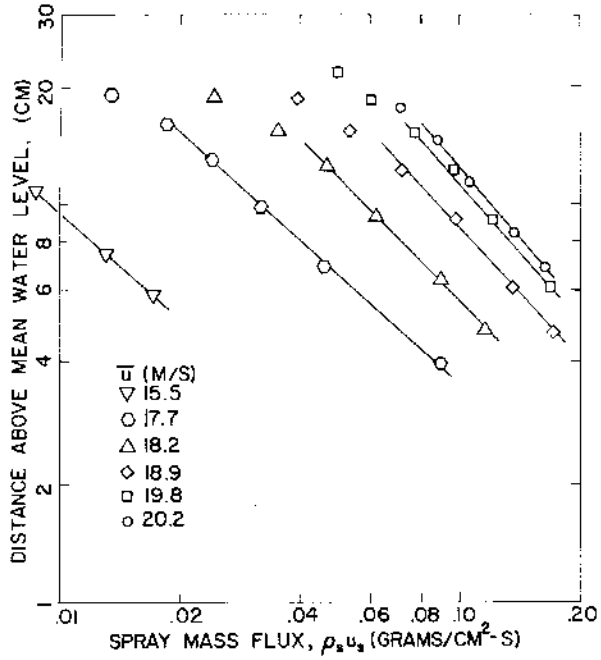

Fig. 5 Mass flux of spray above air-water interface.

The two probes were mounted side by side on a vertically transversing mechanism which could be accurately positioned within ± 0.75 mm, relative to the channel ceiling. Plastic tubing connected the probes to a Validyne differential pressure transducer and the mean velocity was found by low pass filtering the output signal with a cutoff frequency below that of the dominant wave.

Mean velocity profiles were constructed for each wind condition by plotting the measured values of $\langle u(z)\rangle$ vs the logarithm of the probe height above the mean level of the wave troughs. Selection of the wave trough as the appropriate $z=0$ reference level was based on the results of a study of solid sinusoidal waves by Beebe and Cermak.[10] For a high-density roughness ($\lambda=2.45$) they found that the appropriate $z=0$ is midway between crest and trough, while for less dense waves ($\lambda=8.4$), $z=0$ at the trough level. Since $12<\lambda<16$ for the waves in the channel, it was deemed appropriate to set $z=0$ at the average level of the troughs.

Graphed in this way, a logarithmic region exists near the water surface for each of the profiles shown in Fig. 4. The slope of a tangent line through this region is the value of u_*/κ and the intercept at $\langle u\rangle=0$ is the value of the aerodynamic roughness length z_0. These quantities are summarized in Table 1 where the reference velocity u_{10} corresponds to an extrapolation of the tangent line to a height of 10 m. The present

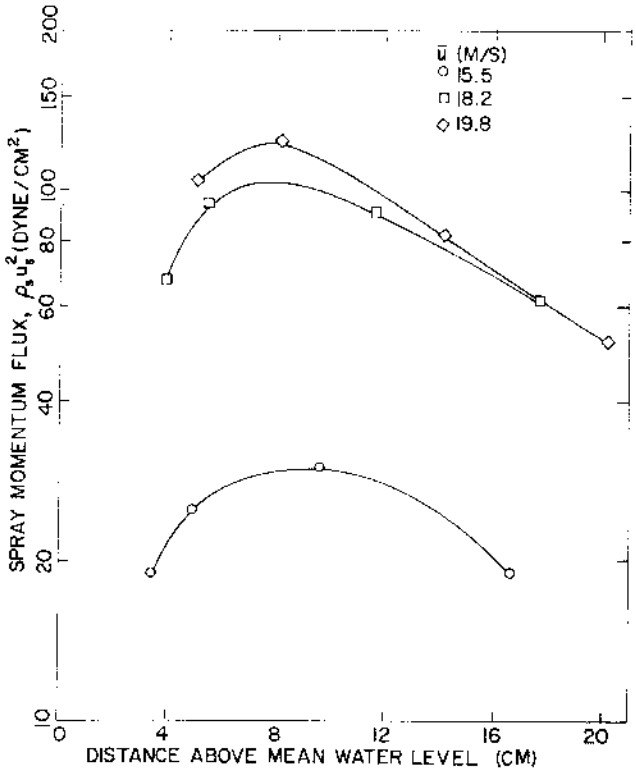

Fig. 6 Momentum flux of spray above air-water interface.

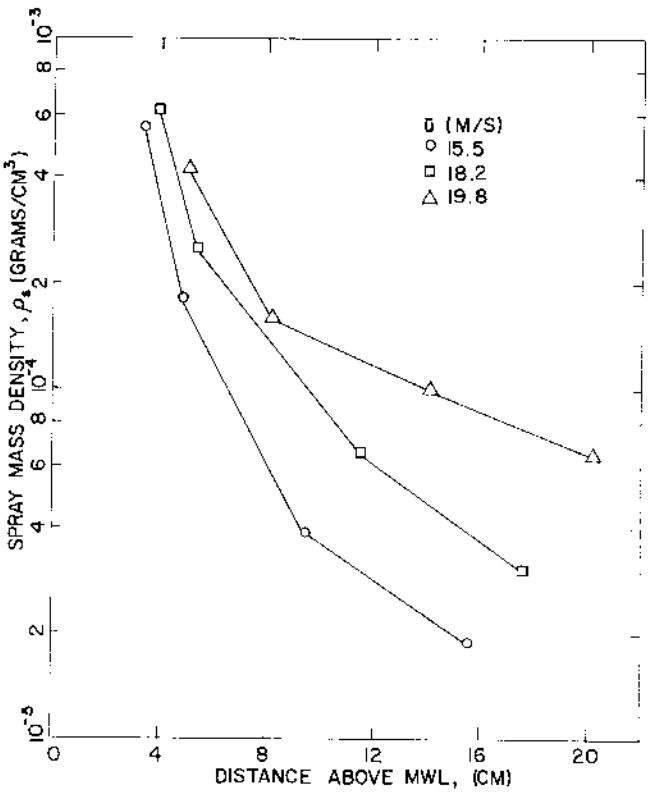

Fig. 7 Mass concentration of spray above air-water interface.

results are in agreement with the laboratory measurements of Toba[18] and Wu[19] for values of u_{i0} up to about 20 m/s, which is the maximum speed attained in those investigations.

Spray Measurements

Measurements involving the spray included the horizontal mass flux of water, the horizontal number flux of spray drops, and the spray impact pressure. Taken together, these

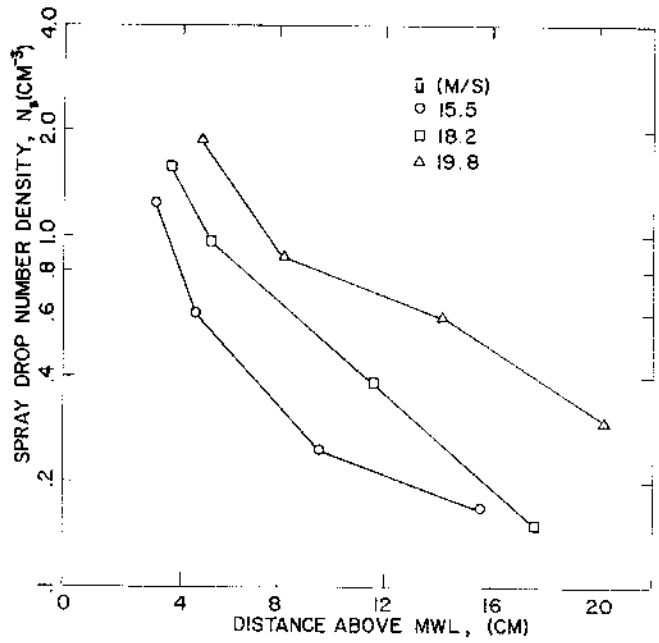

Fig. 8 Number concentration of water drops above air-water interface.

three measurements made possible the determination of the spray mass density, the spray drop number density, and an average spray flux velocity.

The mass flux of water mass was measured with an aspirated sampling probe having a 1.43 cm diam capture area. The air-water mixture captured by the probe was drawn through a cyclone separator at an air volume flow rate of 42 liter/min. At a wind speed of 25 m/s, the isokinetic extraction rate would be 240 liter/min. Considering the relatively large sizes of drops produced in the channel (diam ~ 1.0 mm), it is estimated that the probe capture efficiency was nearly 100%.[20] A stopwatch was used to measure the time required to collect a sample of 25-50 ml of water in the bottom of the separator. Collection times varied 2-20 min, depending on the wind speed and distance above the water surface. The horizontal mass flux of spray is defined as

$$\rho_s u_s = \frac{(\text{volume collected}) \times (\text{water density})}{(\text{collection time}) \times (\text{probe capture area})}$$

The results of vertical traverses with the sampling probe for several wind conditions are presented in Fig. 5. The variation of $\rho_s u_s$ with distance above the mean water level (MWL) is well represented by a power law relationship.

The horizontal number flux of droplets and the spray impact pressure were measured by a Sundstrand Corporation Model 206 Piezotron dynamic pressure transducer. The quartz piezoelectric transducer was mounted to the traversing mechanism with its 0.80 cm diam active surface exposed to the impact of the spray drops. The output signal, which was the voltage analog to the diaphragm pressure time-history of each drop impact, was recorded on magnetic tape for subsequent analysis. The number flux of spray drops was computed from the number of impacts per unit time and the transducer surface area.

Assuming that the droplet trajectories are unaffected by the airflow around the transducer, the time-averaged pressure sensed by the transducer is equal to the momentum flux of the spray, $\rho_s u_s^2$. The recorded signal was digitized and numerically integrated to evaluate this mean spray impact pressure. The real time sampling rate in the analog-to-digital conversion was 65,536 s^{-1} and the time associated with a single impact was approximately 10^{-4} s. The results of the integration are presented in Fig. 6 where the impact pressure or, equivalently, the spray momentum flux, is shown to be a function of both

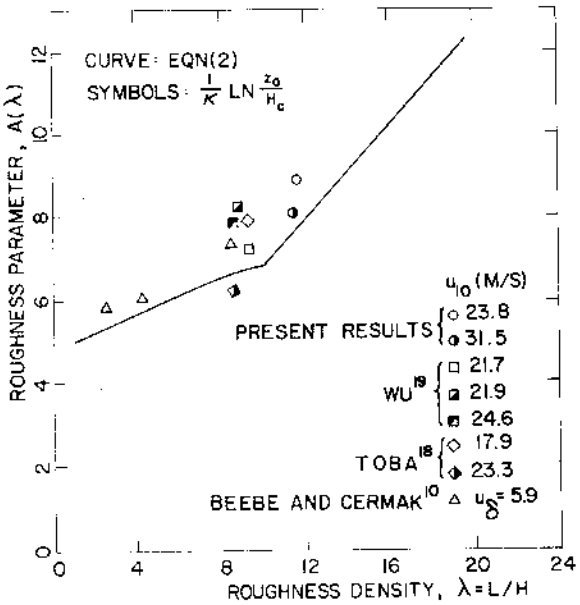

Fig. 9 Log law parameter A as function of wavelength-to-height ratio.

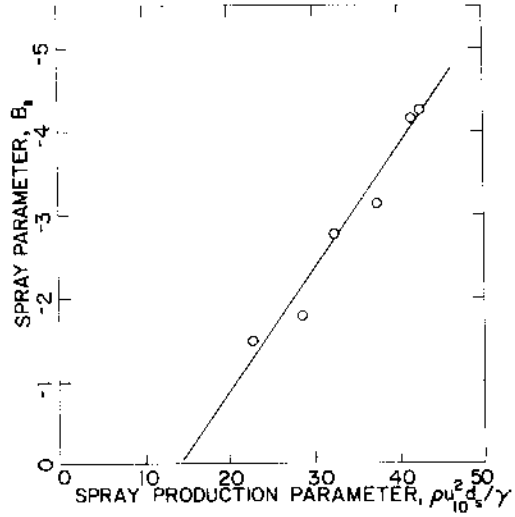

Fig. 10 Log law parameter B_s as function of spray production parameter.

wind speed and elevation. The decrease in $\rho_s u_s^2$ at low elevations can be explained by a low flux velocity u_s, while the decrease at the high elevations is the result of smaller spray concentration ρ_s.

Spray Concentration Distributions

The spray mass density was calculated from the measured values of spray mass flux and momentum flux as

$$\rho_s = (\rho_s u_s)^2 / (\rho_s u_s^2)$$

and the results are presented in Fig. 7 for the three wind speeds at which momentum flux data were taken. Based on the inherent difficulties in the spray measurement techniques described earlier, these values of ρ_s are probably accurate within ±25%. Figure 8 is a similar graph for the number density of drops N_s. At a height of 10 cm, the mass and number densities for the maximum wind condition are approximately 1.2×10^{-4} g/cm^3 and 0.8 drops/cm^3, respectively. As expected, these concentrations are orders of magnitude greater than the concentrations measured in low-wind speed studies previously reported in the literature.[12,21-24] Also computed from the flux measurements were the local spray flux velocity u_s and a characteristic spherical drop diameter d_s, defined by the relation

$$(\pi/6)\rho_w d_s^3 = \rho_s / N_s$$

Analysis of Experimental Results

The Effect of Spray Concentration on κ

An estimate of the effect of water mass content on the value of κ was made, based on the correlation with the power ratio P_s/P_τ discussed earlier. The power P_s was computed by evaluating the integral of Eq. (8), for the experimental data from the heights of the wave crests to the heights of the maximum channel velocities. The available power was approximated from the measured data as

$$P_\tau = \rho (u_*/\kappa)^2 \bar{u} \kappa^2$$

Then, the expressions for the ratio of $\kappa^2 P_s/P_\tau$ were solved simultaneously with the correlation for P_s/P_τ vs κ in Ref. 14. The resulting values of P_s/P_τ are of the order of 10^{-4}, with corresponding values of κ of about 0.37. Since the data points for that portion of the correlation curve are scattered and few, κ is assigned the standard value of 0.4 in the present analysis. Although the mass of water suspended in the air is appreciable, it does not represent a significant portion of the total turbulent energy associated with the wind shear.

Comparison with the Modified Log Law

The proposed model for the mean wind was predicated on the hypothesis that the correlation of Han et al.[9] for the roughness density parameter $A(\lambda)$ can be applied to a wavy water surface. Restating the model

$$\frac{\langle u \rangle}{u_*} = \frac{1}{\kappa} \ln \frac{z}{H_c} + A(\lambda) + B_s$$

From the definition of the log law, it follows that

$$A(\lambda) + B_s = \frac{1}{\kappa} \ln \frac{z_0}{H_c} \tag{15}$$

Considering first the condition when the wind velocity is less than that required for appreciable spray production and entrainment, the spray term B_s should be equal to zero. The right side of Eq. (15) has been evaluated for the available water wave data in this restricted wind speed range (maximum channel velocity ≤ 15 m/s). The present results and those of two previous investigations by Wu[19] and Toba[18] are shown in Fig. 9, along with the function for $A(\lambda)$. While all but one of the experimental points lie somewhat above the correlation, the agreement in both magnitude and trend is good. Also shown in the figure are the data points representing the measurements over solid, sinusoidal boundaries by Beebe and Cermak.[10]

At the higher wind speeds where spray concentrations were appreciable, Eq. (15) was used to evaluate the term B_s assuming that $A(\lambda)$ was still given by Eq. (2). Since B_s represents the increase in surface roughness due to spray production, it should be a function of a Weber number involving the local surface friction force and the surface tension of water. If it is further assumed that the friction force is proportional to the square of the 10 m reference wind velocity, then

$$B_s = \text{function}\left(\frac{\rho u_{10}^2}{\gamma/d_s}\right) \tag{16}$$

where γ is the surface tension and d_s the spray drop diameter. In Fig. 10 the experimental data demonstrate an approximately linear form for Eq. (16).

The Spray Stress

Inherent in the modified log law formulation is the hypothesis that the entrained spray, through the apparent stress term τ_s, represents a significant part of the overall momentum transfer from the wind. The experimental measurements provide two independent estimates of the magnitude of τ_s. First,

Table 2 Fraction of the total drag attributed to τ_s

$\bar{u}$, m/s	$\tau_s/\rho u_*^2$ Eq. (17)	Eq. (19)
15.5	0.13	0.16
17.1	0.16	–
18.2	0.22	0.30
18.9	0.26	–
19.8	0.34	0.36
20.2	0.33	–

the spray stress can be expressed by the difference

$$\tau_s = \rho u_*^2 - \tau_0 \tag{17}$$

where the total momentum flux ρu_*^2 is known from the mean wind profile and τ_0 is given by the log law for the special case of no spray entrainment,

$$\tau_0 = \rho \left[\frac{\langle u - c \rangle}{\frac{1}{\kappa} \ell_n \frac{z}{H} + A(\lambda)} \right]^2 \tag{18}$$

That is, τ_0 is the surface stress of a solid boundary with a geometry identical to the water surface.

The second, independent calculation of τ_s is based on the spray measurements. In terms of the quantities measured, the spray dray force can be estimated if Eq. (4) is approximated as

$$X_s(z) = N_s \rho (\pi d_s^2/8) C_{Ds} (\langle u \rangle - u_s)^2 \tag{19}$$

The spherical drop drag coefficient C_{Ds} is a function of the Reynolds number based on characteristic drop diameter d_s and relative wind speed. Equation (19) was evaluated for the experimental data and integrated from the height of the wave crest to the height of maximum wind velocity, yielding values for τ_s.

The results of the two computations for the ratio of spray stress-to-total stress are compared in Table 2, showing good agreement. At the maximum channel wind velocity, the entrained spray accounted for 30–35% of the total momentum flux through the shear layer.

Conclusions

The effect of spray entrainment on the mean wind profile above a wavy water surface has been treated analytically by including an additional spray stress term in the log law formulation for turbulent boundary-layer flow. The results of measurements in a high-speed wind/wave channel appear to support the modified log law and the partitioning of the vertical momentum flux between separation drag on the wave shape and acceleration of entrained spray.

Successful application of the log law model to the ocean environment depends on correctly defining the aerodynamic roughness of the sea surface. Unlike the laboratory experiment where z_0 was determined by a dominant wave component, the sea surface contains a broad spectrum of wave shapes. It is possible that Kitaigorodskii's[15] suggested use of the wave component with maximum spectral energy density will adequately define the effective wave height. However, the field data to demonstrate this are not available. The data required are simultaneous measurements of wave shapes, mean wind profiles, and spray concentration profiles analogous to those measured in the laboratory.

Within the scope of the present analysis, the following conclusions can be made:

1) The correlation of Han et al.[9] for the roughness parameter $A(\lambda)$ is reasonably applicable to the water wave geometry produced in the wind/wave channel for wind speeds greater than 10 m/s.

2) At the highest wind speed in the wind/wave channel ($\bar{u} = 20$ m/s), the drag force on the entrained spray drops accounted for 30-35% of the overall momentum budget in the shear layer. This result was predicted by the modified log law.

Acknowledgment

This research was sponsored by the National Oceanic and Atmospheric Administration Office of Sea Grant, under Grant 04-7-158-44105.

References

[1] Graff, W.J. and North, R.B., "State of the Art of Fixed Offshore Platforms in the Gulf of Mexico," Dept. of Civil Engineering, University of Houston, Texas, Rept. H-CE-M-45, 1977.

[2] Bretshneider, C.L., "Wave, Tide and Weather Forecasting," *Handbook of Ocean and Underwater Engineering*, edited by J. Myers, McGraw-Hill Book Co., New York, 1969, pp. 11–98.

[3] Plate, E.J., *Aerodynamic Characteristics of Atmospheric Boundary Layers*, AEC Critical Review Series, TID-25465, National Technical Information Service, U.S. Department of Commerce, Springfield, Va., 1972, p. 190.

[4] Hsu, S.A., "A Dynamic Roughness Equation and its Application to Wind Stress Determination at the Air-Sea Interface," *Journal of Physical Oceanography*, Vol. 4, Jan. 1974, pp. 116–120.

[5] Schlicting, H., *Boundary Layer Theory*, 6th ed., McGraw-Hill Book Co., New York, 1968.

[6] Dvorak, F.A., "Calculation of Turbulent Boundary Layers on Rough Surfaces in Pressure Gradient," *AIAA Journal*, Vol. 7, Sept. 1969, pp. 1752–1759.

[7] Simpson, R.L., "A Generalized Correlation of Roughness Density Effects on the Turbulent Boundary Layer," *AIAA Journal*, Vol. 11, Feb. 1972, pp. 242–244.

[8] Furuya, Y., Miyata, M., and Fujita, H., "Turbulent Boundary Layer and Flow Resistance on Plates Roughened by Wires," *Journal of Fluids Engineering*, Vol. 98, Dec. 1976, pp. 635–644.

[9] Han, J.C., Glicksman, L.R., and Rohsenow, W.M., "An Investigation of Heat Transfer and Friction for Rib-Roughened Surfaces," *International Journal of Heat and Mass Transfer*, Vol. 21, 1978, pp. 1143–1156.

[10] Beebe, P.S. and Cermak, J.E., "Turbulent Flow Over a Wavy Boundary," Project Themis, Fluid Mechanics Program, Colorado State University, Fort Collins, Technical Rept. 16, May 1972.

[11] Kraus, E.B., *Atmosphere-Ocean Interaction*, Oxford University Press, London, 1972, p. 275.

[12] Preobrazhenskii, L.Y., "Estimate of the Content of Spray-Drops in the Near-Water Layer of the Atmosphere," *Fluid Mechanics—Soviet Research*, Vol. 2, March–April, 1973, pp. 95–100.

[13] Soo, S.L., "Dynamics of Charged Suspensions," *Topics in Current Aerosol Research*, edited by G.M. Hidy and J.R. Brock, Pergamon Press, New York, 1971, p. 86.

[14] *Sedimentation Engineering*, edited V. Vanoni, Manuals and Reports 54, American Society of Civil Engineers, New York, 1977, pp. 83–91.

[15] Kitaigorodskii, S.A., *The Physics of Air-Sea Interaction*, Israel Program for Scientific Translation, Jerusalem, 1973, p. 32.

[16] Macha, J.M., "The Effects of Sea Spray Entrainment on the Mean Wind Profile and the Overall Load on Marine Structures," Dissertation, Texas A&M University, College Station, 1979.

[17] Welch, P.D., "The Use of Fast Fourier Transform for the Estimation of Power Spectra: A Method Based on Time Averaging over Short, Modified Periodiograms," *IEEE Transactions on Audio and Electroacoustics*, Vol. 15, June 1967, pp. 70–74.

[18] Toba, Y., "Local Balance in the Air-Sea Boundary Process, I: On the Growth Process of Wind Waves," *Journal of the Oceanographical Society of Japan*, Vol. 28, June 1972, pp. 109–121.

[19] Wu, J., "Laboratory Studies of Wind-Wave Interactions," *Journal of Fluid Mechanics*, Vol. 34, Oct. 1968, pp. 91–111.

[20] Dussourd, J.L. and Shapiro, A.H., "A Deceleration Probe for Measuring Stagnation Pressure and Velocity of a Particle-Laden Gas Stream," Heat Transfer and Fluid Mechanics Institute, University of California, Los Angeles, 1955.

[21] Toba, Y., "Drop Production by Bursting of Air Bubbles on the Sea Surface, III: Study by Use of a Wind Flume," *Memoirs of the College of Science*, University of Kyoto, Series A, Vol. 29, No. 3, 1961, pp. 313–344.

[22] Wu., J., "Spray in the Atmospheric Surface Layer: Laboratory Study," *Journal of Geophysical Research*, Vol. 78, Jan. 1973, pp. 511–519.

[23] Lai, R.J. and Shemdin, O.M., "Laboratory Study of the Generation of Spray over Water," *Journal of Geophysical Research*, Vol. 79, July 1974, pp. 3055–3063.

[24] Wang, C.S. and Street, R.L., "Measurements of Spray at an Air-Water Interface," *Dynamics of Atmospheres and Oceans*, Vol. 2, May 1978, pp. 141–152.